Effects of relativity on multiplet splitting and decay rates of the $1s\,2p^2$ configuration of Li-like ions

Mau Hsiung Chen and Bernd Crasemann
Department of Physics and Chemical Physics Institute, University of Oregon, Eugene, Oregon 97403

Hans Mark
National Aeronautics and Space Administration, Washington, D.C. 20546

(Received 1 March 1982)

Properties of the $1s\,2p^2$ states of Li-like ions are calculated relativistically for $6 \leq Z \leq 30$, with particular attention to the effects of the Breit interaction on multiplet splitting and the radiationless transitions through which these states decay. The full Breit interaction (magnetic and retardation terms) is included in calculating fine structure. Transition rates are computed in relativistic intermediate coupling with configuration interaction. Both the spin-orbit and magnetic interactions are incorporated in the calculations. Results are compared with earlier calculations and with experiment, and the physics of observed relativistic and configuration-interaction effects is discussed.

I. INTRODUCTION

Excited states of atoms in the lithium isoelectronic sequence are of special interest because they exhibit the strong relativistic and quantum electrodynamic effects that are characteristic of highly stripped ions, yet these systems are amenable to quite detailed theoretical treatment and experimental study. In particular, the Li-like $1s\,2l\,2l'$ configurations have been studied both experimentally[1–5] and theoretically.[6–13] Their study leads to information that is relevant to transitions in ionic species which occur in astrophysical and plasma milieus, among others.

In a companion paper,[13] we have calculated Auger and x-ray emission rates for the $1s\,2s\,2p$ configuration of Li-like ions, in the intermediate-coupling scheme, with Dirac-Hartree-Slater wave functions and the Møller relativistic two-electron operator. In the present article, we complete the study of $1s\,2l\,2l'$ three-electron configurations by applying relativistic theory to the $1s\,2p^2$ states, with particular attention to the effect of the Breit interaction on multiplet splitting and on the radiationless transitions through which these states decay.

All previous calculations of $1s\,2p^2$-configuration decay probabilities have been nonrelativistic, albeit in intermediate coupling.[6,8–12] Yet, our relativistic $1s\,2s\,2p$ calculations have illustrated the importance of including the magnetic interaction in the Auger transition rate.[13] Cheng *et al.* have shown that the magnetic interaction significantly affects the fine structure of the ^4P_J states of the $1s\,2l\,3l'$ configurations[14]; however, these authors included the (less pronounced) effect of retardation only through the configuration average.

In the present paper, the full Breit interaction (magnetic and retardation terms) is included in calculating fine structure. Radiative and radiationless decay rates of the $1s\,2p^2$ multiplet states are computed for 12 elements ($6 \leq Z \leq 30$) in relativistic intermediate coupling with configuration interaction. Both the spin-orbit and magnetic interactions are incorporated in the calculations. We do not include elements near the neutral end of the Li isoelectronic sequence ($3 \leq Z < 6$) because for these species electron-electron correlations may become so important as to make the present treatment inadequate.

II. THEORY

A. Auger transition rates

The Auger decay probabilities of the multiplet states are calculated from perturbation theory, assuming frozen orbitals.[13,15] The transition rate is

$$T = \frac{2\pi}{\hbar} \left| \left\langle \psi_f \left| \sum_{i<j} V_{ij} \right| \psi_i \right\rangle \right|^2 \rho(\epsilon) \, . \tag{1}$$

Here, ψ_i and ψ_f are the antisymmetrized many-electron wave functions of the initial and final states of the ion, respectively, $\rho(\epsilon)$ is the energy density of final states, and V_{ij} is the two-electron

TABLE I. Fine-structure intervals of the $1s\,2s\,2p\,{}^4P_J$ and $1s\,2p^2\,{}^4P_J$ states in the Li isoelectronic sequence (in cm^{-1}).

	$1s\,2s\,2p\,{}^4P$		$1s\,2p^2\,{}^4P$	
Z	$J=\frac{5}{2}-\frac{3}{2}$	$J=\frac{3}{2}-\frac{1}{2}$	$J=\frac{5}{2}-\frac{3}{2}$	$J=\frac{3}{2}-\frac{1}{2}$
6	94.4	4.4	39.5	74.6
7	208.5	35.1	111.9	158.0
8	404	101	248	296
9	713	211	474	503
10	1 169	389	816	810
13	3 907	1 519	2 939	2 616
18	17 018	6 894	11 487	11 553
20	27 415	10 824	19 305	18 416
22	42 312	15 970	27 904	30 950
25	72 501	24 914	43 476	54 561
26	91 664	30 100	49 108	66 666
30	180 167	48 361	71 136	141 122

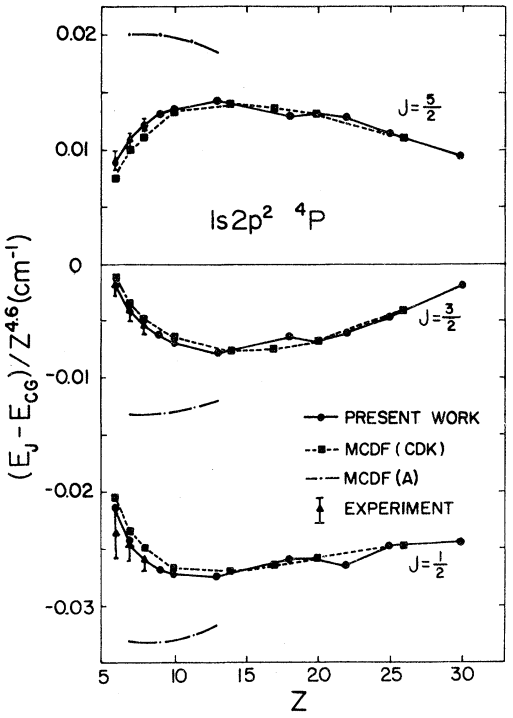

FIG. 1. Separations of the $1s\,2p^2\,{}^4P_J$ levels from the "center-of-gravity" energy of the quartet states, as functions of atomic number Z, scaled by $Z^{-4.6}$. Present relativistic calculations are compared with multiconfigurational Dirac-Fock results in which the Breit energy is included in the configuration-averge energy only [MCDF (A), Ref. 22] and in which the magnetic energy (but not retardation) is included in the splitting calculation [MCDF (CDK), Ref. 14]. Experimental data from Ref. 4 are indicated as well.

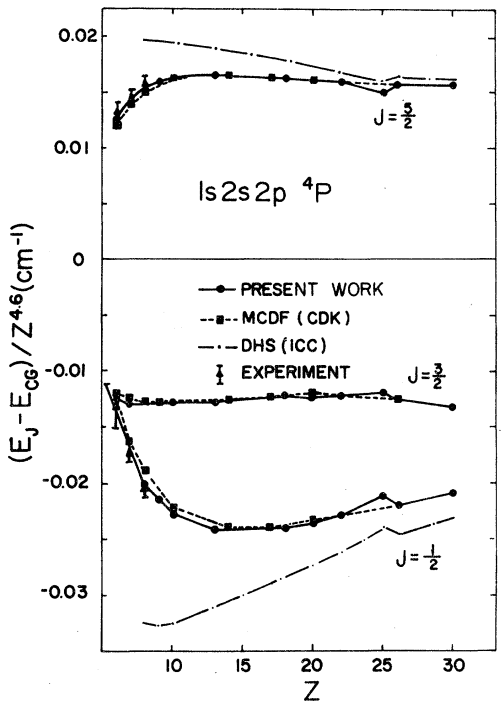

FIG. 2. Separations of the $1s\,2s\,2p\,{}^4P_J$ levels from the "center-of-gravity" energy of the quartet states, as functions of atomic number Z, scaled by $Z^{-4.6}$. Present relativistic calculations are compared with a Dirac-Hartree-Slater computation in intermediate coupling in which the Breit energy is included in the configuration-average energy only [DHS (ICC), Ref. 13, extended in the present work] and in which the magnetic energy (but not retardation) is included in the splitting calculation [MCDF (CDK), in Ref. 14]. Experimental data from Ref. 4 are also indicated.

TABLE II. Radiative transition energies (in eV) betweeen the centers of gravity of the $1s\,2p^2\,{}^4P$ and $1s\,2s\,2p\,{}^4P$ states.

	Theory		
Z	Present	MCDF[a]	Experiment[b]
6	9.266	9.357	9.224±0.002
7	11.208	11.302	11.159±0.001
8	13.144	13.260	13.095±0.001
9	14.968		
10	16.938	17.232	
13	23.666		
18	34.875		
20	39.987	40.544	
22	46.725		
25	55.856		
26	60.196	59.723	
30	74.618		

[a]Reference 14.
[b]Reference 4.

interaction operator for which the Møller operator is chosen[15,16]:

$$V_{ij}=(1-\vec{\alpha}_i\cdot\vec{\alpha}_j)\exp(i\omega r_{ij})/r_{ij}\ . \tag{2}$$

This operator includes the retarded Coulomb and the current-current interactions. The $\vec{\alpha}_i$ are Dirac matrices, and ω is the wave number of the virtual photon.

The restricted Dirac-Fock wave functions have the standard form[17]

$$\psi_{n\kappa m}(r)=\frac{1}{r}\begin{bmatrix} G_{n\kappa}(r)\Omega_{\kappa m} \\ iF_{n\kappa}(r)\Omega_{-\kappa m}\end{bmatrix}. \tag{3}$$

Here, $G_{n\kappa}$ and $F_{n\kappa}$ are the large and small components of the relativistic radial wave functions, respectively, and Ω denotes the angular wave functions.

The Auger matrix elements in j-j coupling can then be separated by Racah algebra into angular parts multiplied by radial integrals. For a detailed derivation, the reader is referred to our previous work.[13,15]

B. X-ray emission rates

From first-order perturbation theory, the emission of a photon of energy $\hbar\omega$ and momentum $\hbar k$ into a solid-angle element $d\Omega$, with polarization vector $\hat{\epsilon}$, by an atom going from an initial state i to a final state f, is given by

$$T_{fi}=\frac{\alpha\omega}{2\pi}\left|\left\langle\psi_f\left|\sum_j\vec{\alpha}_j\cdot\hat{\epsilon}e^{i\vec{\kappa}_j\cdot\vec{r}_j}\right|\psi_i\right\rangle\right|^2 d\Omega\ , \tag{4}$$

where

$$\hbar\omega=\hbar kc=E_i-E_f\ . \tag{5}$$

We follow the procedure of earlier calculations[18–21] by multipole expansion of the plane-wave radiation field. The multiplet x-ray matrix element is separated into angular parts and radial integrals by using Racah algebra. Details are described in Ref. 13.

C. Relativistic intermediate coupling

We use the j-j coupled states as basis states. The mixing of states with the same total angular

TABLE III. Calculated K Auger energies (in eV) for the $1s\,2p^2$ configuration of Li-like ions.

	Initial state							
Z	$^2S_{1/2}$	$^2P_{1/2}$	$^2P_{3/2}$	$^2D_{3/2}$	$^2D_{5/2}$	$^4P_{1/2}$	$^4P_{3/2}$	$^4P_{5/2}$
6	249.24	243.31	243.33	242.61	242.59	238.28	238.28	238.29
7	339.61	332.66	332.69	331.65	331.63	326.27	326.29	326.30
8	443.96	435.99	436.06	434.68	434.64	428.24	428.27	428.31
9	561.97	552.96	553.08	551.36	551.31	543.84	543.91	543.96
10	693.42	683.39	683.59	681.51	681.44	672.90	673.00	673.10
13	1171.14	1157.87	1158.55	1155.32	1155.19	1143.27	1143.59	1143.96
18	2244.31	2224.74	2227.73	2221.79	2221.80	2203.17	2204.61	2206.03
20	2771.75	2748.67	2753.96	2745.91	2746.49	2724.27	2726.55	2728.94
22	3355.10	3327.89	3336.34	3325.64	3327.16	3300.32	3304.15	3307.61
25	4338.86	4303.67	4318.90	4302.41	4306.72	4271.08	4277.85	4283.24
26	4697.80	4659.28	4677.55	4658.52	4664.26	4624.69	4632.95	4339.04
30	6274.31	6218.54	6253.27	6220.25	6235.40	6173.34	6190.83	6199.65

TABLE IV. Calculated K x-ray energies (in eV) for the $1s2p^2$ configuration of Li-like ions.

Transition[a]	Atomic number 6	7	8	9	10	13	18	20	22	25	26	30
$^2P_{1/2}$-$^2S_{1/2}$	305.35	427.41	570.15	733.03	916.49	1591.30	3129.98	3892.13	4740.45	6172.93	6694.28	8999.06
$^2P_{3/2}$-$^2S_{1/2}$	305.33	427.38	570.08	732.91	916.46	1590.59	3126.82	3887.09	4732.78	6159.52	6677.96	8970.18
$^2P_{1/2}$-$^2P_{1/2}$	299.42	420.46	562.18	724.01	906.46	1578.03	3110.41	3869.05	4713.24	6137.74	6655.76	8943.29
$^2P_{3/2}$-$^2P_{1/2}$	299.40	420.43	562.11	723.89	906.43	1577.32	3107.26	3864.01	4705.57	6124.32	6639.44	8914.41
$^2P_{1/2}$-$^2P_{3/2}$	299.43	420.50	562.25	724.13	906.66	1578.71	3113.40	3874.34	4721.68	6152.97	6674.04	8978.02
$^2P_{3/2}$-$^2P_{3/2}$	299.42	420.46	562.18	724.02	906.63	1578.00	3110.25	3869.30	4714.01	6139.56	6657.72	8949.14
$^2P_{1/2}$-$^2D_{3/2}$	298.71	419.45	560.87	722.41	904.59	1575.48	3107.45	3866.29	4710.99	6136.48	6655.00	8945.00
$^2P_{3/2}$-$^2D_{3/2}$	298.70	419.42	560.81	722.29	904.56	1574.77	3104.30	3861.25	4703.32	6123.07	6638.68	8916.12
$^2P_{3/2}$-$^2D_{5/2}$	298.69	419.40	560.77	722.24	904.49	1474.64	3104.32	3861.83	4704.84	6127.37	6644.43	8931.28
$^2P_{1/2}$-$^4P_{1/2}$	294.38	414.07	554.43	714.89	895.98	1563.43	3088.84	3844.65	4685.67	6105.15	6621.17	8898.09
$^2P_{3/2}$-$^4P_{1/2}$	294.37	414.04	554.36	714.78	895.95	1562.72	3085.69	3839.61	4677.99	6091.74	6604.85	8869.21
$^2P_{1/2}$-$^4P_{3/2}$	294.39	414.09	554.46	714.96	896.08	1563.76	3090.27	3846.93	4689.50	6111.91	6629.44	8915.59
$^2P_{3/2}$-$^4P_{3/2}$	294.38	414.06	554.40	714.84	896.05	1563.04	3087.12	3841.89	4681.83	6098.50	6613.12	8886.71
$^2P_{3/2}$-$^4P_{5/2}$	294.38	414.07	554.43	714.90	896.15	1563.41	3088.54	3844.28	4685.29	6103.89	6619.21	8895.53

[a]Following convention, the higher-energy state is listed second.

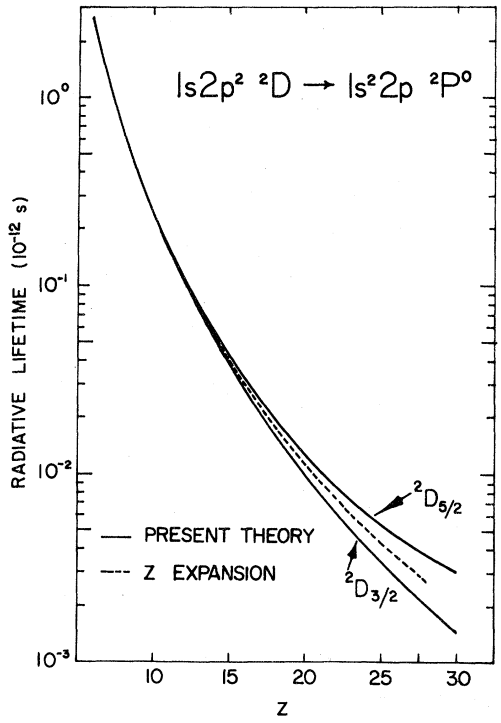

FIG. 3. K radiative lifetimes of $1s2p^2\,^2D$ states, as functions of atomic number Z. Present theoretical results are compared with those from Z-expansion theory (Ref. 23).

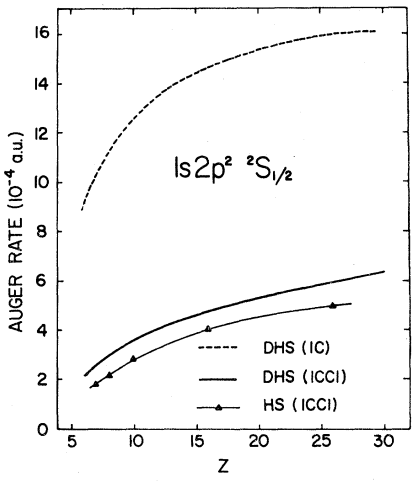

FIG. 4. Auger decay rate of the $1s2p^2\,^2S$ state, as a function of atomic number Z. Results from a Dirac-Hartree-Slater calculation in intermediate coupling [DHS (IC)] are compared with relativistic [DHS (ICCI)] and nonrelativistic [HS (ICCI), Ref. 11] calculations that include configuration interaction.

TABLE V. Comparison between theoretical and experimental x-ray energies of $1s\,2p^2 \rightarrow 1s^2 p_{1/2,3/2}$ transitions (all energies in eV).

Transitions	$Z=20$		$Z=22$		$Z=26$	
$(1s^2 2p\text{-}1s\,2p^2)$	Theory[a]	Experiment[b]	Theory[a]	Experiment[b]	Theory[a]	Experiment[b]
$^2P_{1/2}$-$^2S_{1/2}$			4740.5	4739.2	6694.3	6692.9
$^2P_{3/2}$-$^2S_{1/2}$			4732.8	4731.5	6678.0	6676.9
$^2P_{1/2}$-$^2P_{3/2}$	3874.3	3875.9	4721.7	4722.8	6674.0	6675.1
$^2P_{3/2}$-$^2P_{3/2}$	3869.3	3870.8	4714.0	4715.1	6657.7	6659.2
$^2P_{1/2}$-$^2D_{3/2}$	3866.3	3867.6	4711.0	4710.8		
$^2P_{3/2}$-$^2D_{3/2}$	3861.3	3862.5	4703.3	4703.1		
$^2P_{3/2}$-$^2D_{5/2}$	3861.8	3862.8	4704.8	4704.4	6644.4	6644.3

[a]Present work.
[b]Reference 24.

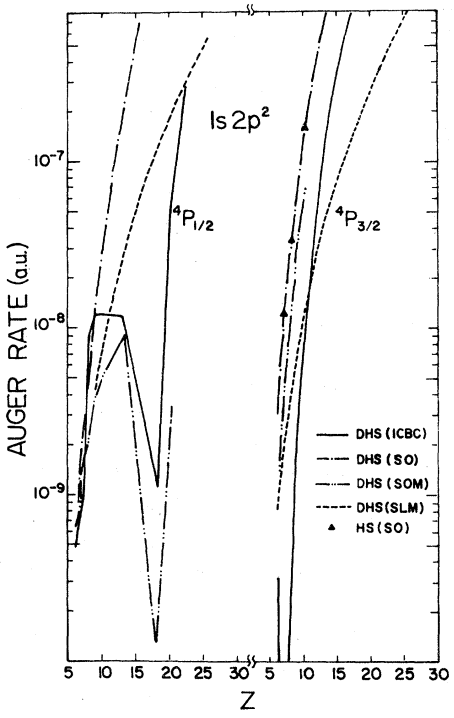

FIG. 5. Auger decay rates of $1s\,2p^2\,{}^4P_{1/2}$ and $^4P_{3/2}$ states, as functions of atomic number Z. The following relativistic calculations from the present work are shown: DHS (ICBC) in intermediate coupling, with the Breit and Coulomb interactions included in the energy matrix from which the mixing coefficients are computed, both Coulomb and magnetic interactions included in the Auger matrix element; DHS (SO) with the spin-orbit interaction only in the energy matrix from which the mixing coefficients are computed, and with the Coulomb interaction only in the Auger matrix element; DHS (SOM) same as DHS (SO) but with the magnetic interaction included in the Auger matrix element; DHS (SLM) no mixing; pure LS states, but the magnetic interaction is included in the Auger matrix element. For comparison, nonrelativistic results from Ref. 11 are shown as well [HS (SO)], which are analogous to DHS (SO) but for the use of nonrelativistic Hartree-Slater orbitals.

momentum, due to the residual Coulomb and transverse interactions, is then included. For the $1s\,2p^2$ initial configuration, the states of total angular momentum $J=\frac{1}{2}$, $J=\frac{3}{2}$, and $J=\frac{5}{2}$, respectively, contain the following admixtures:

$J=\frac{1}{2}$

$$
\begin{aligned}
&(1)\ 1s,2s^2(0);\tfrac{1}{2}\ ,\\
&(2)\ 1s,2p^2_{1/2}(0);\tfrac{1}{2}\ ,\\
&(3)\ 1s,2p^2_{3/2}(0);\tfrac{1}{2}\ ,\\
&(4)\ 1s,2p_{1/2}2p_{3/2}(1);\tfrac{1}{2}\ ,
\end{aligned}
\qquad (6)
$$

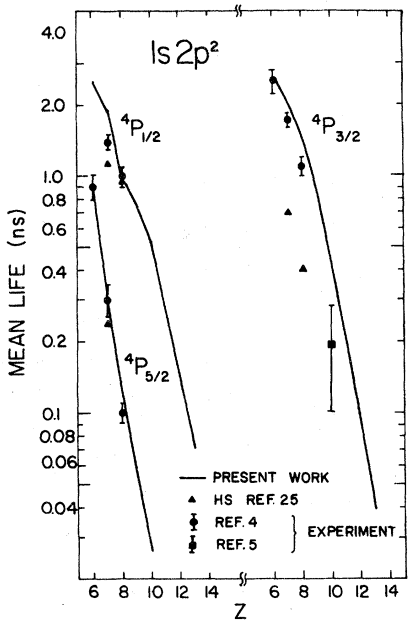

FIG. 6. Lifetimes of the $1s\,2p^2\,{}^4P$ states. The present relativistic results are compared with nonrelativistic HS calculations from Ref. 25 and with experimental data from Refs. 4 and 5.

TABLE VI. Theoretical Auger and x-ray emission rates (in a.u.[a]) for the $^2S_{1/2}$, $^2P_{1/2}$, and $^2P_{3/2}$ states of the $1s\,2p^2$ configuration of Li-like ions.

	$^2S_{1/2}$			$^2P_{1/2}$			$^2P_{3/2}$		
Z	Auger	$1s$-$2p_{1/2}$	$1s$-$2p_{3/2}$	Auger	$1s$-$2p_{1/2}$	$1s$-$2p_{3/2}$	Auger	$1s$-$2p_{1/2}$	$1s$-$2p_{3/2}$
6	2.085(−4)	2.776(−6)	5.644(−6)	8.099(−9)	1.913(−5)	9.522(−6)	4.195(−7)	4.582(−6)	2.406(−5)
7	2.599(−4)	5.745(−6)	1.184(−5)	2.171(−8)	3.984(−5)	1.975(−5)	1.021(−6)	9.350(−6)	5.021(−5)
8	2.913(−4)	1.069(−5)	2.235(−5)	3.171(−8)	7.463(−5)	3.684(−5)	2.260(−6)	1.702(−5)	9.434(−5)
9	3.190(−4)	1.791(−5)	3.846(−5)	7.395(−8)	1.275(−4)	6.247(−5)	4.683(−6)	2.803(−5)	1.616(−4)
10	3.484(−4)	2.806(−5)	6.246(−5)	1.591(−7)	2.047(−4)	9.930(−5)	9.00(−6)	4.293(−5)	2.603(−4)
13	4.127(−4)	7.924(−5)	2.083(−4)	8.856(−7)	6.544(−4)	3.030(−4)	4.455(−5)	1.102(−4)	8.374(−4)
18	4.866(−4)	2.217(−4)	9.593(−4)	5.928(−6)	2.711(−3)	1.102(−3)	2.249(−4)	2.456(−4)	3.403(−3)
20	5.122(−4)	2.659(−4)	1.610(−3)	1.094(−5)	4.288(−3)	1.610(−3)	3.842(−4)	2.443(−4)	5.238(−3)
22	5.344(−4)	2.847(−4)	2.578(−3)	1.794(−5)	6.452(−3)	2.235(−3)	5.255(−4)	2.373(−4)	7.659(−3)
25	5.682(−4)	2.859(−4)	4.767(−3)	3.067(−5)	1.100(−2)	3.463(−3)	7.137(−4)	2.025(−4)	1.258(−2)
26	5.782(−4)	2.719(−4)	5.747(−3)	3.539(−5)	1.290(−2)	3.951(−3)	7.655(−4)	1.877(−4)	1.461(−2)
30	6.191(−4)	1.902(−4)	1.112(−2)	5.303(−5)	2.235(−2)	6.497(−3)	9.136(−4)	1.309(−4)	2.516(−2)

[a]We have 1 a.u.$=27.21$ eV$/\hbar=4.134\times10^{16}$ sec^{-1}. Numbers in parentheses stand for powers of ten, e.g., $2.085(-4)=2.085\times10^{-4}$.

$J=\frac{3}{2}$

(1) $1s,2p^2_{3/2}(2);\frac{3}{2}$,

(2) $1s,2p_{1/2}2p_{3/2}(1);\frac{3}{2}$, (7)

(3) $1s,2p_{1/2}2p_{3/2}(2);\frac{3}{2}$,

$J=\frac{5}{2}$

(1) $1s,2p^2_{3/2}(2);\frac{5}{2}$,

(2) $1s,2p_{1/2}2p_{3/2}(2);\frac{5}{2}$. (8)

The basis states for the $1s\,2s\,2p$ configuration are listed in Ref. 13.

The eigenfunctions and eigenvalues are found by diagonalizing the energy matrices, which include not only the Coulomb interaction but also the transverse interaction. These eigenfunctions and eigenvalues are then used to calculate the multiplet splitting, Auger and x-ray energies, and the transition rates. The mixing coefficients of the states enumerated in Eqs. (6)—(8) are listed in the Appendix.

III. NUMERICAL CALCULATIONS

The relativistic Auger and x-ray matrix elements in j-j coupling were calculated from Dirac-Hartree-Slater (DHS) wave functions that correspond to the appropriate initial electron configurations. The transition energies were found by performing separate self-consistent-field calculations for the initial and final configurations, thus including relaxation energies. Contributions due to the Breit interaction, vacuum polarization, and K-shell self-energy were also included in the energy calculations. The Coulomb and Breit-interaction matrix elements required for the intermediate-coupling calculations were evaluated with the slightly modified general Auger program.[15]

For transitions from initial doublet states, we calculate the x-ray and Auger matrix elements with average energies pertaining to the entire configuration. The decay rates of quartet states are more energy sensitive, hence we use energies corresponding to the center of gravity of only the quartet states in computing their decay.

IV. RESULTS AND DISCUSSION

A. Multiplet splitting

The theoretical multiplet splitting of the ^4P_J ($J=\frac{1}{2},\frac{3}{2},\frac{5}{2}$) states of the $1s\,2p^2$ and $1s\,2s\,2p$ config-

TABLE VII. Theoretical Auger and x-ray emission rates (in a.u.) for the $^2D_{3/2}$ and $^2D_{5/2}$ states of the $1s2p^2$ configuration of Li-like ions.

	$^2D_{3/2}$			$^2D_{5/2}$		
Z	Auger	$1s$-$2p_{1/2}$	$1s$-$2p_{3/2}$	Auger	$1s$-$2p_{1/2}$	$1s$-$2p_{3/2}$
6	2.195(−3)	8.145(−6)	1.404(−6)	2.198(−3)	2.649(−13)	9.552(−6)
7	2.497(−3)	1.712(−5)	2.750(−6)	2.503(−3)	1.118(−12)	1.987(−5)
8	2.710(−3)	3.245(−5)	4.729(−6)	2.720(−3)	3.925(−12)	3.716(−5)
9	2.901(−3)	5.629(−5)	7.200(−6)	2.915(−3)	1.119(−11)	6.334(−5)
10	3.043(−3)	9.198(−5)	9.914(−6)	3.064(−3)	2.817(−11)	1.014(−4)
13	3.301(−3)	3.148(−4)	1.374(−5)	3.363(−3)	2.662(−10)	3.192(−4)
18	3.410(−3)	1.456(−3)	1.095(−6)	3.644(−3)	3.780(−9)	1.268(−3)
20	3.317(−3)	2.405(−3)	5.241(−5)	3.668(−3)	8.229(−9)	1.945(−3)
22	3.226(−3)	3.709(−3)	2.023(−4)	3.649(−3)	1.611(−8)	2.831(−3)
25	3.091(−3)	6.509(−3)	7.240(−4)	3.505(−3)	3.553(−8)	4.527(−3)
26	3.050(−3)	7.706(−3)	9.984(−4)	3.424(−3)	4.380(−8)	5.171(−3)
30	2.937(−3)	1.410(−2)	2.693(−3)	3.005(−3)	8.021(−8)	8.000(−3)

urations are listed in Table I. These fine-structure intervals are compared in Figs. 1 and 2 with experimental and other theoretical results. Severe discrepancies exist between experimental data and the results of calculations which include the Breit energy in the configuration-average energy only, regardless of whether a multiconfigurational Dirac-Fock (MCDF) (Ref. 22) or DHS (Ref. 13) approach with intermediate coupling is used. Drastic improvement in the agreement between theory and experiment is attained when the magnetic energy is included in the splitting calculations, even without the retardation correction.[4,14] The present work, which includes the full Breit interaction (magnetic and retardation) in the correctly coupled state calculations, leads to excellent agreement with experiment.

B. Transition energies

Radiative transitions from $1s2p^2\,^4\mathrm{P}$ initial to $1s2s2p\,^4P$ final states have been observed by Livingston and Berry in beam-foil spectra.[4] The theoretical and experimental x-ray transition energies between centers of gravity of $1s2p^2\,^4P$ and $1s2s2p\,^4P$ states are compared in Table II. The MCDF results[14] were obtained including the magnetic interaction correctly in the energy calculations, but incorporating the retardation term only in the configuration average. In the present results, the full Breit interaction is included for each state. Table II shows that retardation contributes little to the radiative transition energies but is nonnegligible.

Our calculated K Auger and x-ray energies are listed in Tables III and IV. The present K x-ray energies agree to ~ 1 eV with results from Z-expansion theory.[8,23] In Table V, we compare our K x-ray energies with experimental results.[1,24] In general, the present calculations agree with the data to within ~ 1.5 eV. The residual error is probably due to correlation, which has mostly been neglected in this work.

C. Transition rates

The theoretical radiative and Auger transition rates from the present work are listed in Tables VI–VIII. For the ^2S and ^2D states, Auger rates from nonrelativistic Hartree-Slater (HS) calculations[6,10–11] do not differ materially from the present relativistic results. However, Auger rates from calculations using Coulomb wave functions[8] are quite different from those based on self-consistent-field models.

The K x-ray emission rates of the doublet states are quite close to earlier results from the nonrelativistic HS (Refs. 6, 10, and 11) or Z-expansion[8,23] theory. In Fig. 3, we compare K radiative lifetimes of ^2D states from the present calculations with results from the Z-expansion theory.[23] For $Z \gtrsim 15$, the effect of the spin-orbit interaction becomes quite important. Thus, x-ray decay rates of the $^2D_{3/2}$ and $^2D_{5/2}$ states begin to differ, and at $Z \cong 30$, the radiative lifetime of the $^2D_{5/2}$ state is twice that of the $^2D_{3/2}$ state.

There is strong configuration interaction between the $1s2p^2\,^2S$ and $1s2s^2\,^2S$ states: The Auger decay rate of the former is reduced by a factor of ~ 3 due

TABLE VIII. Theoretical Auger and x-ray emission rates (in a.u.) for the $^4P_{1/2}$, $^4P_{3/2}$, and $^4P_{5/2}$ states of the $1s\,2p^2$ configuration of Li-like ions.

	$^4P_{1/2}$				$^4P_{3/2}$				$^4P_{5/2}$			
Z	Auger	1s-2$p_{1/2}$	1s-2$p_{3/2}$	2s-2p	Auger	1s-2$p_{1/2}$	1s-2$p_{3/2}$	2s-2p	Auger	1s-2$p_{1/2}$	1s-2$p_{3/2}$	2s-2p
6	4.896(−10)	6.213(−11)	1.179(−12)	8.928(−9)	3.149(−10)	1.310(−11)	1.186(−10)	8.941(−9)	1.813(−8)	1.342(−13)	1.040(−10)	8.963(−9)
7	9.471(−10)	3.354(−10)	9.823(−12)	1.110(−8)	4.635(−11)	4.327(−11)	6.065(−10)	1.113(−8)	5.956(−8)	5.712(−13)	5.956(−10)	1.117(−8)
8	8.847(−9)	1.285(−9)	1.595(−11)	1.329(−8)	1.694(−10)	1.289(−10)	2.480(−9)	1.334(−8)	1.625(−7)	1.956(−12)	2.652(−9)	1.343(−8)
9	1.183(−8)	4.790(−9)	9.737(−11)	1.538(−8)	2.303(−9)	3.235(−10)	8.521(−9)	1.547(−8)	3.835(−7)	5.686(−12)	9.720(−9)	1.561(−8)
10	1.194(−8)	1.556(−8)	4.490(−10)	1.766(−8)	1.006(−8)	7.057(−10)	2.534(−8)	1.781(−8)	8.112(−7)	1.466(−11)	3.074(−8)	1.804(−8)
13	1.169(−8)	2.716(−7)	1.088(−8)	2.579(−8)	1.409(−7)	4.774(−9)	3.726(−7)	2.629(−8)	5.064(−6)	1.534(−10)	5.304(−7)	2.704(−8)
18	1.139(−9)	9.541(−6)	1.888(−7)	4.139(−8)	1.266(−6)	5.337(−8)	8.162(−6)	4.394(−8)	4.076(−5)	2.888(−9)	1.521(−5)	4.691(−8)
20	5.147(−8)	2.940(−5)	7.473(−7)	4.933(−8)	3.020(−6)	1.023(−7)	2.466(−5)	5.393(−8)	9.742(−5)	7.906(−9)	5.469(−5)	5.835(−8)
22	2.623(−7)	9.257(−5)	1.145(−6)	5.990(−8)	5.051(−6)	2.189(−7)	5.880(−5)	6.827(−8)	1.841(−4)	1.971(−8)	1.504(−4)	7.464(−8)
25	1.340(−6)	3.351(−4)	3.014(−6)	7.591(−8)	8.960(−6)	6.787(−7)	1.786(−4)	9.424(−8)	4.090(−4)	6.812(−8)	5.528(−4)	1.034(−7)
26	2.060(−6)	5.088(−4)	3.389(−6)	8.315(−8)	1.038(−5)	9.869(−7)	2.479(−4)	1.073(−7)	5.115(−4)	9.973(−8)	8.075(−4)	1.175(−7)
30	7.955(−6)	2.151(−3)	2.797(−6)	1.076(−7)	1.536(−5)	4.320(−6)	7.708(−4)	1.709(−7)	1.009(−3)	3.882(−7)	2.810(−3)	1.828(−7)

to this effect (Fig. 4). The $1s\,2s^2\,{}^2S$ admixture to the $1s\,2p^2\,{}^2S$ state amounts to 12% for $Z=6$ and slowly decreases with Z to 5% at $Z=30$. The Auger decay rate of the $1s\,2s^2\,{}^2S$ state is approximately one order of magnitude larger than that of the $1s\,2p^2\,{}^2S$ states; consequently, an important effect of the admixture on the Auger rate persists even for heavier elements.

For the ^2P states, Auger decay is forbidden in the nonrelativistic limit in LS coupling. These states decay primarily by K x-ray emission. The Auger decay of these states gains strength, however, from mixing with other doublet states through intermediate coupling.

For the ^4P states, both Auger and dipole K x-ray transitions are forbidden in the nonrelativistic approximation. The quartet states can decay radiatively only by magnetic-quadrupole ($M2$) K x-ray emission, or by electric-dipole ($E1$) transitions made possible by mixing with doublet states through intermediate coupling or by $1s\,2p^2\,{}^4P \rightarrow 1s\,2s\,2p\,{}^4P$ $E1$ transitions. Auger decay of the ^4P states can occur through mixing with doublet states or by the magnetic interaction. Contributions from the magnetic interaction to the ^4P Auger decay grow with atomic number roughly as $Z^{4.7}$; contributions due to mixing with doublet states through the spin-orbit interaction grow as $\sim Z^7$. The Z dependence of the 2s-2p $E1$ transition intensity is found to be as $\sim Z^{1.7}$. In the present calculations, all of these decay modes are included for the ^4P_J states. The $M2$ radiative transition rates are found to be smaller than the $E1$ rates made possible by mixing with doublet states. For low-Z atoms, $E1$ transitions of the 2s-2p type are the dominant decay modes of the $^4P_{1/2}$ and $^4P_{3/2}$ states, while the $^4P_{5/2}$ states decay predominantly through Auger transitions made possible by mixing with doublet states.

The 2s-2p radiative transitions are characterized by small transition energies and rates, whence they are sensitive to differences in the atomic model. In the present work, the 2s-2p $E1$ transitions are calculated in the Coulomb gauge, which corresponds to the dipole-velocity form in the nonrelativistic dipole approximation. The nonrelativistic calculations,[12,25] on the other hand, have been performed in the dipole-length approximation. This difference might account for the large discrepancies between present 2s-2p x-ray rates and results from nonrelativistic theory.[12,25]

For the Auger decay of the $^4P_{1/2}$ and $^4P_{3/2}$ states, contributions from the magnetic interaction are as important as contributions due to mixing

TABLE IX. Mixing coefficients of the $J=\frac{1}{2}$ states of the $1s\,2p^2$ configuration of Li-like ions [Eq. (6)].

		Basis			
Z	State	(1)	(2)	(3)	(4)
6	$^2S_{1/2}$	−0.343 91	0.539 99	0.768 21	0.000 83
	$^2P_{1/2}$	0.000 99	−0.471 86	0.331 25	0.817 08
	$^4P_{1/2}$	−0.001 06	0.667 95	−0.470 61	0.576 52
7	$^2S_{1/2}$	−0.338 47	0.539 43	0.771 01	0.001 57
	$^2P_{1/2}$	0.001 76	−0.472 40	0.329 62	0.817 43
	$^4P_{1/2}$	−0.001 84	0.668 84	−0.469 93	0.576 03
8	$^2S_{1/2}$	−0.333 80	0.538 47	0.773 71	0.002 45
	$^2P_{1/2}$	0.003 10	−0.472 82	0.327 81	0.817 91
	$^4P_{1/2}$	−0.003 70	0.669 72	−0.469 51	0.575 34
9	$^2S_{1/2}$	−0.332 47	0.535 55	0.776 29	0.003 88
	$^2P_{1/2}$	0.004 55	−0.473 83	0.324 74	0.818 54
	$^4P_{1/2}$	−0.005 22	0.671 36	−0.468 27	0.574 43
10	$^2S_{1/2}$	−0.328 18	0.532 18	0.780 41	0.005 86
	$^2P_{1/2}$	0.006 35	−0.475 23	0.320 58	0.819 36
	$^4P_{1/2}$	−0.006 96	0.673 55	−0.466 54	0.573 25
13	$^2S_{1/2}$	−0.319 30	0.514 47	0.795 70	0.014 94
	$^2P_{1/2}$	0.014 55	−0.481 10	0.301 45	0.823 08
	$^4P_{1/2}$	−0.015 24	0.683 43	−0.458 66	0.567 73
18	$^2S_{1/2}$	−0.301 18	0.461 14	0.833 69	0.040 04
	$^2P_{1/2}$	0.035 68	−0.489 30	0.243 55	0.836 71
	$^4P_{1/2}$	−0.038 91	0.714 51	−0.435 51	0.546 16
20	$^2S_{1/2}$	−0.289 79	0.426 30	0.855 20	0.054 11
	$^2P_{1/2}$	0.047 21	−0.491 60	0.207 63	0.844 39
	$^4P_{1/2}$	−0.054 11	0.733 78	−0.417 84	0.532 97
22	$^2S_{1/2}$	−0.277 36	0.387 01	0.876 71	0.068 37
	$^2P_{1/2}$	0.057 90	−0.482 70	0.164 47	0.858 25
	$^4P_{1/2}$	−0.072 16	0.760 06	−0.398 01	0.508 62
25	$^2S_{1/2}$	−0.255 15	0.332 22	0.904 21	0.083 26
	$^2P_{1/2}$	0.067 70	−0.461 96	0.108 01	0.877 69
	$^4P_{1/2}$	−0.096 64	0.797 33	−0.363 67	0.471 87
26	$^2S_{1/2}$	−0.247 09	0.312 77	0.912 97	0.087 23
	$^2P_{1/2}$	0.069 70	−0.449 20	0.088 06	0.886 35
	$^4P_{1/2}$	−0.105 94	0.812 01	−0.350 29	0.454 66
30	$^2S_{1/2}$	−0.212 74	0.240 27	0.942 39	0.094 43
	$^2P_{1/2}$	0.068 50	−0.377 45	0.019 18	0.923 29
	$^4P_{1/2}$	−0.141 52	0.869 92	−0.291 03	0.372 18

with doublet states through intermediate coupling. Consequently, it is essential to include the magnetic interaction in the Auger calculations for the $1s\,2p^2\,{}^4P_{1/2,3/2}$ states. In previous nonrelativistic calculations,[6,8–12] contributions of the magnetic interaction were not included. Since strong cancellations occur between contributions from the mixing with doublet states and from the magnetic interaction, the Auger rates of the $^4P_{1/2,3/2}$ states are very sensitive to details of the atomic model and to the transition energies. In the intermediate-coupling calculations, inclusion of the magnetic interaction in the energy matrix can change the decay rates of these states by one whole order to magnitude (Fig. 5). Average transition energies of quartet states, rather than configuration-average energies, were employed in the present calculations for quartet states. Results differ from those of nonrelativistic Auger-rate calculations[6,8–12] for the $^4P_{1/2,3/2}$ states by as much as two orders of magnitude (Fig. 5).

For the $^4P_{5/2}$ state, mixing with $^2D_{5/2}$ contributes much more to the Auger rate than the magnetic interaction. Consequently, the present relativistic $^4P_{5/2}$ Auger-decay rates do not differ significantly from nonrelativistic results.[6,8–12]

Comparing the lifetimes of the ^4P_J states from the present relativistic calculations with results from nonrelativistic theory[25] and experimental

TABLE X. Mixing coefficients of the $J=\frac{3}{2}$ states of the $1s\,2p^2$ configuration of Li-like ions [Eq. (7)].

		Basis		
Z	State	(1)	(2)	(3)
6	$^2P_{3/2}$	0.754 91	−0.406 36	−0.514 77
	$^2D_{3/2}$	0.565 79	0.006 59	0.824 52
	$^4P_{3/2}$	0.331 66	0.913 69	−0.234 88
7	$^2P_{3/2}$	0.759 25	−0.405 29	−0.509 19
	$^2D_{3/2}$	0.560 60	0.009 91	0.828 03
	$^4P_{3/2}$	0.330 55	0.914 13	−0.234 73
8	$^2P_{3/2}$	0.765 16	−0.403 82	−0.501 46
	$^2D_{3/2}$	0.553 41	0.014 45	0.832 79
	$^4P_{3/2}$	0.329 05	0.914 72	−0.234 54
9	$^2P_{3/2}$	0.772 47	−0.401 88	−0.491 71
	$^2D_{3/2}$	0.544 34	0.020 24	0.838 62
	$^4P_{3/2}$	0.327 08	0.915 47	−0.234 39
10	$^2P_{3/2}$	0.781 40	−0.399 39	−0.479 47
	$^2D_{3/2}$	0.532 95	0.027 44	0.845 70
	$^4P_{3/2}$	0.324 61	0.916 37	−0.234 30
13	$^2P_{3/2}$	0.817 72	−0.387 15	−0.425 97
	$^2D_{3/2}$	0.482 67	0.057 96	0.873 88
	$^4P_{3/2}$	0.313 63	0.920 19	−0.234 26
18	$^2P_{3/2}$	0.887 00	−0.349 14	−0.302 21
	$^2D_{3/2}$	0.362 65	0.121 58	0.923 96
	$^4P_{3/2}$	0.285 85	0.929 15	−0.234 45
20	$^2P_{3/2}$	0.918 90	−0.319 79	−0.231 01
	$^2D_{3/2}$	0.291 22	0.154 84	0.944 04
	$^4P_{3/2}$	0.266 12	0.934 75	−0.235 41
22	$^2P_{3/2}$	0.939 66	−0.292 29	−0.177 79
	$^2D_{3/2}$	0.235 93	0.177 29	0.955 46
	$^4P_{3/2}$	0.247 76	0.939 75	−0.235 55
25	$^2P_{3/2}$	0.961 39	−0.250 09	−0.114 81
	$^2D_{3/2}$	0.167 51	0.200 80	0.965 20
	$^4P_{3/2}$	0.218 34	0.947 17	−0.234 94
26	$^2P_{3/2}$	0.966 70	−0.236 31	−0.098 25
	$^2D_{3/2}$	0.148 70	0.206 17	0.967 15
	$^4P_{3/2}$	0.208 29	0.949 55	−0.234 44
30	$^2P_{3/2}$	0.981 30	−0.185 59	−0.051 14
	$^2D_{3/2}$	0.091 77	0.217 42	0.971 75
	$^4P_{3/2}$	0.169 22	0.958 27	−0.230 38

TABLE XI. Mixing coefficients of the $J=\frac{5}{2}$ states of the $1s\,2p^2$ configuration of Li-like ions [Eq. (8)].

		Basis	
Z	State	(1)	(2)
6	$^2D_{5/2}$	0.579 86	0.814 72
	$^4P_{5/2}$	0.814 72	−0.579 86
7	$^2D_{5/2}$	0.581 57	0.813 50
	$^4P_{5/2}$	0.813 50	−0.581 57
8	$^2D_{5/2}$	0.583 94	0.811 79
	$^4P_{5/2}$	0.811 79	−0.583 94
9	$^2D_{5/2}$	0.587 07	0.809 54
	$^4P_{5/2}$	0.809 54	−0.587 07
10	$^2D_{5/2}$	0.591 05	0.806 63
	$^4P_{5/2}$	0.806 63	−0.591 05
13	$^2D_{5/2}$	0.609 45	0.792 83
	$^4P_{5/2}$	0.792 83	−0.609 45
18	$^2D_{5/2}$	0.661 62	0.749 84
	$^4P_{5/2}$	0.749 84	−0.661 62
20	$^2D_{5/2}$	0.703 08	0.711 11
	$^4P_{5/2}$	0.711 11	−0.703 08
22	$^2D_{5/2}$	0.744 46	0.667 67
	$^4P_{5/2}$	−0.667 67	0.744 46
25	$^2D_{5/2}$	0.812 73	0.582 64
	$^4P_{5/2}$	−0.582 64	0.812 73
26	$^2D_{5/2}$	0.835 36	0.549 70
	$^4P_{5/2}$	−0.549 70	0.835 36
30	$^2D_{5/2}$	0.911 37	0.411 59
	$^4P_{5/2}$	−0.411 59	0.911 37

data,[4,5] we find that the relativistic results agree much better with experiment (Fig. 6).

Configuration interaction between the $1s\,2p^2\,^4P$ states and ^4P states of other configurations (e.g., $1s\,3p^2\,^4P$, $1s\,3d^2\,^4P$) is not expected to affect the Auger rates appreciably, because these other ^4P states are also Auger forbidden in the nonrelativistic limit. However, in view of the sensitivity of the $^4P_{1/2,3/2}$ Auger rates to the fine details of the atomic model, it may well be that inclusion of full exchange in the continuum as well as bound-state wave functions could be important. MCDF calculations to explore this question are in progress.

ACKNOWLEDGMENT

This work was supported in part by the Air Force Office of Scientific Research under Grant No. 79-0026.

APPENDIX: MIXING COEFFICIENTS

In Tables IX–XI we list the eigenfunction coefficients that describe the mixing of the states in Eqs. (6)–(8).

[1]V. A. Boiko, A. Ya Faenov, and S. A. Pikuz, J. Quant. Spectrosc. Radiat. Transfer 19, 11 (1978).

[2]E. Ya Gol'ts, U. I. Zitnik, E. Ya Kononov, S. L. Mandel'shtam, and Yu V. Sidel'nikov, Dokl. Akad. Nauk SSSR 220, 560 (1975) [Sov. Phys.—Dokl. 20, 49 (1975)].

[3]E. V. Aglitsky, V. A. Boiko, S. M. Zaharov, S. A. Pikuz, and A. Yu Faenov, Kvant. Electron. (Moscow) 1, 908 (1974) [Sov. J. Quantum Electron. 4, 500 (1974)].

[4]A. E. Livingston and H. G. Berry, Phys. Rev. A 17, 1966 (1978).

[5]S. Schumann, K.-O. Groeneveld, G. Nolte, and B. Fricke, Z. Phys. A 289, 245 (1979).

[6]C. P. Bhalla, A. H. Gabriel, and L. P. Presnyakov, Mon. Not. R. Astron. Soc. 172, 359 (1975).

[7]K. T. Cheng, C. P. Lin, and W. R. Johnson, Phys. Lett. A 48, 437 (1974); and private communication.

[8]L. A. Vainshtein and U. I. Safronova, At. Data Nucl. Data Tables 21, 50 (1978).

[9]A. H. Gabriel, Mon. Not. R. Astron. Soc. 160, 99 (1972).

[10]M. H. Chen and B. Crasemann, Phys. Rev. A 12, 959 (1975).

[11]C. P. Bhalla and A. H. Gabriel, in *Beam-Foil Spectroscopy,* edited by I. A. Sellin and D. J. Pegg (Plenum, New York, 1976), Vol. 1, p. 121.

[12]F. Bely-Dubau, J. Dubau, P. Faucher, and L. Steenman-Clark, J. Phys. B 14, 3313 (1981).

[13]M. H. Chen, B. Crasemann, and H. Mark, Phys. Rev. A 24, 1852 (1981).

[14]K. T. Cheng, J. P. Desclaux, and Y.-K. Kim, J. Phys. B 11, L359 (1978).

[15]M. H. Chen, E. Laiman, B. Crasemann, M. Aoyagi, and H. Mark, Phys. Rev. 19, 2253 (1979).

[16]C. Møller, Ann. Phys. (Leipzig) 14, 531 (1932).

[17]M. E. Rose, *Relativistic Electron Theory* (Wiley, New York, 1961).

[18]J. H. Scofield, in *Atomic Inner-Shell Processes,* edited by B. Crasemann (Academic, New York, 1975), Vol. I, p. 265.

[19]J. H. Scofield, Phys. Rev. 179, 9 (1969).

[20]H. R. Rosner and C. P. Bhalla, Z. Phys. 231, 347 (1970).

[21]I. P. Grant, J. Phys. B 7, 1458 (1974).

[22]Calculation with I. P. Grant's MCDF program; Comput. Phys. Commun. 21, 207 (1980).

[23]J. L. Fox and A. Dalgarno, Phys. Rev. A 16, 283 (1977).

[24]J. Sugar and C. Corliss, J. Phys. Chem. Ref. Data 8, 1 (1979); 8, 865 (1979); 4, 353 (1975).

[25]Calculated by C. P. Bhalla, quoted in Ref. 4.